SKEWED PARTON DISTRIBUTIONS*

A.V. RADYUSHKIN†

Physics Department, Old Dominion University
Norfolk, VA 23529, USA
and
Jefferson Lab, Newport News,VA 23606, USA

(Received November 11, 1999)

Applications of perturbative QCD to deeply virtual Compton scattering and hard exclusive electroproduction processes require a generalization of usual parton distributions for the case when long-distance information is accumulated in nonforward matrix elements of quark and gluon light-cone operators. We describe two types of nonperturbative functions parametrizing such matrix elements: double distributions $F(x,y;t)$ and skewed distribution functions $\mathcal{F}_\zeta(X;t)$, discuss their properties, and basic uses in the QCD description of hard exclusive processes.

PACS numbers: 12.38.Bx, 13.60.Fz, 13.60.Le

1. Introduction

The standard feature of applications of perturbative QCD to hard processes is the introduction of phenomenological functions accumulating information about nonperturbative long-distance dynamics. The well-known examples are the parton distribution functions $f_{p/H}(x)$ [1] used in perturbative QCD approaches to hard inclusive processes and distribution amplitudes $\varphi_\pi(x)$, $\varphi_N(x_1,x_2,x_3)$, which naturally emerge in the asymptotic QCD analyses of hard exclusive processes [2–7].

The cases of deeply virtual Compton scattering (DVCS) and hard exclusive electroproduction processes [8–13] involve nonforward matrix elements $\langle p'|\ldots|p\rangle$. The important feature (noticed long ago [14,15]) is that kinematics of hard elastic electroproduction processes (DVCS can be also treated as one of them) requires the presence of the longitudinal component in the momentum transfer $r \equiv p - p'$ from the initial hadron to the final: $r^+ = \zeta p^+$.

* Presented at the XXXIX Cracow School of Theoretical Physics, Zakopane, Poland, May 29–June 8, 1999.

† Also at Laboratory of Theoretical Physics, JINR, Dubna, Russia

For DVCS and ρ-electroproduction in the region $Q^2 \gg |t|, m_H^2$, the longitudinal momentum asymmetry (or "skewedness") parameter ζ coincides with the Bjorken variable $x_{Bj} = Q^2/2(pq)$ associated with the virtual photon momentum q [16]. This means that the nonperturbative matrix element $\langle p'| \dots |p\rangle$ is nonsymmetric (skewed), and the distributions which appear in the hard elastic electroproduction amplitudes differ from those studied in inclusive processes. In the latter case, one has a symmetric situation when the same momentum p appears in both brackets of the hadronic matrix element $\langle p| \dots |p\rangle$.

To parametrize nonforward matrix elements $\langle p - r \,|\, \mathcal{O}(0,z) \,|\, p\rangle \,|_{\,z^2=0}$ of quark and gluon light-cone operators one can use two basic types of nonperturbative functions. The double distributions (DDs) $\tilde{F}(x,y;t)$ [9,11,17,18] specify the Sudakov light-cone "plus" fractions xp^+ and yr^+ of the initial hadron momentum p and the momentum transfer r carried by the initial parton. The other possibility is to treat the proportionality coefficient ζ as an independent parameter and introduce an alternative description in terms of the nonforward parton distributions (NFPDs) $\mathcal{F}_\zeta(X;t)$ with $X = x + y\zeta$ being the total fraction of the initial hadron momentum taken by the initial parton. The shape of NFPDs explicitly depends on the parameter ζ characterizing the *skewedness* of the relevant nonforward matrix element. This parametrization of nonforward matrix elements by $\mathcal{F}_\zeta(X;t)$ is similar to that proposed by Ji [8] who introduced off-forward parton distributions (OFPDs) $H(\tilde{x},\xi;t)$ in which the parton momenta and the skewedness parameter $\xi \equiv r^+/2P^+$ are measured in units of the average hadron momentum $P = (p+p')/2$. OFPDs and NFPDs [11,12] can be treated as particular forms of *skewed* parton distributions (SPDs). One can also introduce the version of DDs ("α-DDs" [18]) in which the active parton momentum is written in terms of symmetric variables $k = xP + (1+\alpha)r/2$.

The basics of the pQCD approaches incorporating skewed parton distributions were formulated in Refs. [8–11]. A detailed analysis of pQCD factorization for hard meson electroproduction processes was given in Ref. [12]. Our goal in the present lectures is to give a description of the approach outlined in our papers [9–11,17,18].

2. Double distributions and their symmetries

In the pQCD factorization treatment of hard electroproduction processes, the nonperturbative information is accumulated in the nonforward matrix elements $\langle p-r \,|\, \mathcal{O}(0,z) \,|\, p\rangle$ of light cone operators $\mathcal{O}(0,z)$. For $z^2 = 0$ the matrix elements depend on the relative coordinate z through two Lorentz invariant variables (pz) and (rz). In the forward case, when $r = 0$, one obtains the usual quark helicity-averaged densities by Fourier transforming the

relevant matrix element with respect to (pz)

$$\langle p,s' \mid \bar{\psi}_a(0)\hat{z}E(0,z;A)\psi_a(z) \mid p,s\rangle \mid_{z^2=0}$$
$$= \bar{u}(p,s')\hat{z}u(p,s)\int\limits_0^1 \left(\mathrm{e}^{-ix(pz)}f_a(x) - \mathrm{e}^{ix(pz)}f_{\bar{a}}(x)\right)\,dx\,, \qquad (1)$$

where $E(0,z;A)$ is the gauge link, $\bar{u}(p',s'), u(p,s)$ are the Dirac spinors and we use the notation $\gamma_\alpha z^\alpha \equiv \hat{z}$.

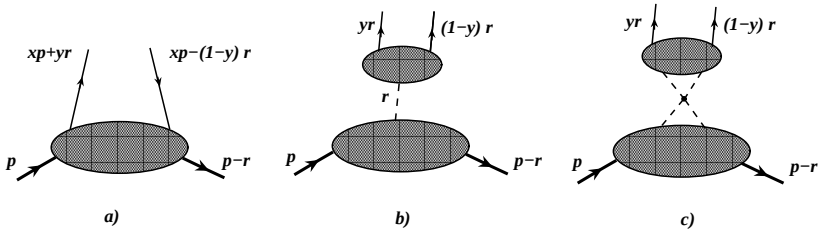

Fig. 1. a) Parton picture in terms of y-DDs; b,c) F_M-type contributions.

The parameter x in this representation has an evident interpretation: it characterizes the fraction of the initial hadron momentum which is carried by the active parton.

In the nonforward case, we can use the double Fourier representation with respect to both (pz) and (rz):

$$\langle p',s' \mid \bar{\psi}_a(0)\hat{z}E(0,z;A)\psi_a(z) \mid p,s\rangle \mid_{z^2=0}$$
$$= \int\limits_0^1 dy \int\limits_{-1}^1 \mathrm{e}^{-ix(pz)-iy(rz)} \left\{\bar{u}(p',s')\hat{z}u(p,s)\,\tilde{F}_a(x,y;t)\right.$$
$$\left. + \bar{u}(p',s')\frac{\hat{z}\hat{r}-\hat{r}\hat{z}}{4M}u(p,s)\,\tilde{K}_a(x,y;t)\right\}\theta(0\le x+y\le 1)\,dx$$
$$+\frac{(zr)}{M}\,\bar{u}(p',s')u(p,s)\int\limits_0^1 \mathrm{e}^{-iy(rz)}\,\Psi_a(y;t)\,dy\,, \qquad (2)$$

where M is the nucleon mass and s,s' specify the nucleon polarization. We use the "hat" (rather than "slash") convention $\hat{z} \equiv z^\mu\gamma_\mu$. The parametrization of nonforward matrix elements must include both the nonflip term described here by the functions $\tilde{F}_a(x,y;t)$ and the spin-flip term characterized by the functions $\tilde{K}_a(x,y;t)$.

The parameters x, y tell us that the active parton carries the fractions x of the initial momentum p and the fraction y of the momentum transfer r. Using the approach [19] based on the α-representation analysis it is possible to prove [11] that double distributions $\tilde{F}(x,y)$ have a natural property that both x and y satisfy the "parton" constraints $0 \le x \le 1$, $0 \le y \le 1$ for any Feynman diagram contributing to $\tilde{F}(x,y)$. A less obvious restriction $0 \le x+y \le 1$ guarantees that the argument $X = x + y\zeta$ of the skewed distribution $\mathcal{F}_\zeta(X)$ also changes between the limits $0 \le X \le 1$. The support area for the *double distribution* $\tilde{F}_a(x,y;t)$ is shown on Fig. 2a.

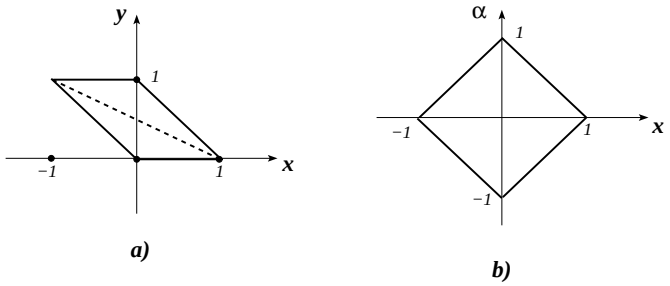

Fig. 2. a) Support region and symmetry line $y = \bar{x}/2$ for y-DDs $\tilde{F}(x,y;t)$; b) support region for α-DDs $\tilde{f}(x,\alpha)$.

In principle, we cannot exclude also the possibility that the functions $\tilde{F}(x,y;t)$ have singular terms at $x=0$ proportional to $\delta(x)$ or its derivative(s). Such terms have no projection onto the usual parton densities. We will denote them by $\tilde{F}_M(x,y;t)$ – they may be interpreted as coming from the t-channel meson-exchange type contributions (see Fig. 1b). In this case, the partons just share the plus component of the momentum transfer r: information about the magnitude of the initial hadron momentum is lost if the exchanged particle can be described by a pole propagator $\sim 1/(t-m_M^2)$. Hence, the meson-exchange contributions to a double distribution may look like

$$\tilde{F}^+_M(x,y;t) \sim \delta(x)\,\frac{\varphi^+_M(y)}{m_M^2 - t} \quad \text{or} \quad \tilde{F}^-_M(x,y;t) \sim \delta'(x)\,\frac{\varphi^-_M(y)}{m_M^2 - t} \quad , \quad etc., \quad (3)$$

where $\varphi^\pm_M(y)$ are the functions related to the distribution amplitudes of the relevant mesons $M^\pm$. The two examples above correspond to x-even and x-odd parts of the double distribution $\tilde{F}(x,y;t)$. Another type of terms in which the dependence on (pz) is lost can be produced by diagrams containing a quartic pion vertex (Fig. 1c). As shown by Polyakov and Weiss [20], such terms correspond to an independent $(rz)\bar{u}(p',s')u(p,s)\Phi((rz))$ type

contribution which can be parametrized by a single integral over y involving an effective distribution amplitude $\Psi(y;t)$. The meson-exchange terms in $\tilde{F}(x,y;t)$ and $\tilde{K}(x,y;t)$ as well as Polyakov–Weiss terms are invisible in the forward limit, hence the existing knowledge of the usual parton densities cannot be used to constrain these terms. Later, describing the models for skewed distributions, we discuss only the "forward visible parts" of SPDs which are obtained by scanning the $x \neq 0$ parts of the relevant DDs.

Comparing Eq. (1) with the $r = 0$ limit of the DD definition (2) gives the "reduction formulas" relating the double distribution $\tilde{F}_a(x,y;t=0)$ to the quark and antiquark parton densities

$$\int\limits_0^{1-x} \tilde{F}_a(x,y;t=0)|_{x>0}\, dy = f_a(x)\ ;\ \int\limits_{-x}^{1} \tilde{F}_a(x,y;t=0)|_{x<0}\, dy = -f_{\bar{a}}(-x)\,. \tag{4}$$

Hence, the positive-x and negative-x components of the double distribution $\tilde{F}_a(x,y;t)$ can be treated as nonforward generalizations of quark and antiquark densities, respectively. If we define the "untilded" DDs by

$$F_a(x,y;t) = \tilde{F}_a(x,y;t)|_{x>0}\ ;\ F_{\bar{a}}(x,y;t) = -\tilde{F}_a(-x,1-y;t)|_{x<0}\,, \tag{5}$$

then x is always positive and the reduction formulas have the same form

$$\int\limits_0^{1-x} F_{a,\bar{a}}(x,y;t=0)|_{x\neq 0}\, dy = f_{a,\bar{a}}(x) \tag{6}$$

in both cases. The new antiquark distributions also "live" on the triangle $0 \leq x,y \leq 1$, $0 \leq x+y \leq 1$. Taking z in the lightcone "minus" direction, we arrive at the parton interpretation of functions $F_{a,\bar{a}}(x,y;t)$ as probability amplitudes for an outgoing parton to carry the fractions xp^+ and yr^+ of the external momenta r and p. The double distributions $F(x,y;t)$ are universal functions describing the flux of p^+ and r^+ independently of the ratio r^+/p^+. Note, that extraction of two separate components $F_a(x,y;t)$ and $F_{\bar{a}}(x,y;t)$ from the quark DD $\tilde{F}_a(x,y;t)$ as its positive-x and negative-x parts is unambiguous.

Taking the $O(z)$ term of the Taylor expansion gives the sum rules

$$\int\limits_0^1 dx \int\limits_0^{1-x} \left[F^a(x,y;t) - F^{\bar{a}}(x,y;t)\right]\, dy = F_1^a(t)\,, \tag{7}$$

$$\int\limits_0^1 dx \int\limits_0^{1-x} \left[K^a(x,y;t) - K^{\bar{a}}(x,y;t)\right]\, dy = F_2^a(t)\,, \tag{8}$$

relating the double distributions $F_a(x,y;t)$, $K_a(x,y;t)$ to the a-flavor components of the Dirac and Pauli form factors:

$$\sum_a e_a F_1^a(t) = F_1(t) \quad , \quad \sum_a e_a F_2^a(t) = F_2(t)\,, \tag{9}$$

respectively.

A common element of the reduction formulas given above is an integration over y. Hence, it is convenient to introduce intermediate functions

$$\mathcal{F}^a(x;t) = \int\limits_0^{1-x} F^a(x,y;t)\,dy\,; \quad \mathcal{K}^a(x;t) = \int\limits_0^{1-x} K^a(x,y;t)\,dy\,. \tag{10}$$

They satisfy the reduction formulas

$$\mathcal{F}^a(x;t=0) = f_a(x)\,; \quad \sum_a e_a \int\limits_0^1 \left[\mathcal{F}^a(x;t) - \mathcal{F}^{\bar a}(x;t)\right]\,dx = F_1(t) \tag{11}$$

$$\sum_a e_a \int\limits_0^1 \left[\mathcal{K}^a(x;t) - \mathcal{K}^{\bar a}(x;t)\right]\,dx = F_2(t) \tag{12}$$

which show that these functions are the simplest hybrids of the usual parton densities and form factors. For this reason, one can call them *nonforward parton densities* (NDs) [21].

The spin-flip terms disappear only if $r = 0$. In the weaker $r^2 \equiv t = 0$ limit, they survive, *e.g.*, $F_2^a(0) = \kappa^a$ is the a-flavor contribution to the nucleon anomalous magnetic moment. In other words, the $t = 0$ limit of the "magnetic" NDs exists: $\mathcal{K}^a(x;t=0) \equiv k_a(x)$, and the integral

$$\sum_a e_a \int\limits_0^1 \left[k_a(x) - k_{\bar a}(x)\right]\,dx = \kappa_p \tag{13}$$

gives the anomalous magnetic moment of the proton. The knowledge of the x-moment of $k_a(x)$'s is needed to determine the contribution of the quark orbital angular momentum to the proton spin [8]. Since the K-type DDs are always accompanied by the $r_\mu = p_\mu - p'_\mu$ factor, they are invisible in deep inelastic scattering and other inclusive processes related to strictly forward $r = 0$ matrix elements.

There are also parton-helicity sensitive double distributions $G^a(x,y;t)$ and $P^a(x,y;t)$. The first one reduces to the usual spin-dependent densities

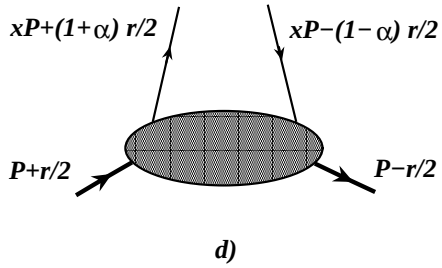

Fig. 3. Parton picture in terms of α-DDs

$\Delta f_a(x)$ in the $r = 0$ limit and gives the axial form factor $F_A(t)$ after the x, y-integration. The second one involves hadron helicity flip and is related to the pseudoscalar form factor $F_P(t)$.

It is worth mentioning here that for a massive target (nucleons in our case) there is a kinematic restriction [16]

$$-t > \frac{\zeta^2 M^2}{\bar{\zeta}}\,. \tag{14}$$

Hence, for fixed ζ, the formal limit $t \to 0$ is not physically reachable. However, many results (evolution equations being the most important example) obtained in the formal $t = 0$, $M = 0$ limit are still applicable.

To make the description more symmetric with respect to the initial and final hadron momenta, we can treat nonforward matrix elements as functions of (Pz) and (rz), where $P = (p + p')/2$ is the average hadron momentum. The relevant double distributions $\tilde{f}_a(x, \alpha\,; t)$ [which we will call α-DDs to distinguish them from y-DDs $F(x, y; t)$] are defined by

$$\begin{aligned}&\left\langle p' \left| \bar{\psi}_a\left(-\frac{z}{2}\right) \hat{z} \psi_a\left(\frac{z}{2}\right) \right| p \right\rangle \\ &= \bar{u}(p')\hat{z}u(p) \int\limits_{-1}^{1} dx \int\limits_{-1+|x|}^{1-|x|} \mathrm{e}^{-ix(Pz)-i\alpha(rz)/2}\, \tilde{f}_a(x, \alpha; t)\, d\alpha \;+ O(r) \text{ terms}\,.\end{aligned} \tag{15}$$

The support area for $\tilde{f}_a(x, \alpha; t)$ is shown in Fig. 2b. Again, the usual forward densities $f_a(x)$ and $f_{\bar{a}}(x)$ are given by integrating $\tilde{f}_a(x, \alpha\,;\, t = 0)$ over vertical lines $x = \text{const}$ for $x > 0$ and $x < 0$, respectively. Hence, we can split $\tilde{f}_a(x, \alpha\,;\, t)$ into three components

$$\tilde{f}_a(x, \alpha\,;\, t) = f_a(x, \alpha\,;\, t)\,\theta(x > 0) - f_{\bar{a}}(-x, -\alpha\,;\, t)\,\theta(x < 0) + f_M(x, \alpha\,;\, t)\,, \tag{16}$$

where $f_M(x,\alpha\,;\,t)$ is a singular term with support at $x = 0$ only. Due to hermiticity and time-reversal invariance properties of nonforward matrix elements, the α-DDs are even functions of α:

$$\tilde{f}_a(x,\alpha;t) = \tilde{f}_a(x,-\alpha;t)\,.$$

For our original y-DDs $F_{a,\bar{a}}(x,y;t)$, this corresponds to symmetry with respect to the interchange $y \leftrightarrow 1-x-y$ ("Munich" symmetry, established in Ref. [22]). In particular, the functions $\varphi_M^{\pm}(y)$ for singular contributions $F_M^{\pm}(x,y;t)$ are symmetric $\varphi_M^{\pm}(y) = \varphi_M^{\pm}(1-y)$ both for x-even and x-odd parts. The a-quark contribution into the flavor-singlet operator

$$\mathcal{O}_a^S\left(-\frac{z}{2},\frac{z}{2}\right) = \frac{i}{2}\left[\bar{\psi}_a\left(-\frac{z}{2}\right)\hat{z}E\left(-\frac{z}{2},\frac{z}{2};A\right)\psi_a\left(\frac{z}{2}\right) - \{z\to -z\}\right]$$

can be parametrized either by y-DDs $\tilde{F}_a^S(x,y;t)$ or by α-DDs $\tilde{f}_a^S(x,\alpha\,;\,t)$

$$\begin{aligned}
&\langle\, p',s' \mid \mathcal{O}_a^S\left(-\frac{z}{2},\frac{z}{2}\right) \mid p,s\rangle \,|_{\,z^2=0}\\
&= \bar{u}(p',s')\hat{z}u(p,s)\int\limits_0^1 dx \int\limits_0^{1-x}\frac{1}{2}\Big(\mathrm{e}^{-ix(pz)-i(y-1/2)(rz)}\\
&\qquad\qquad -\mathrm{e}^{ix(pz)+i(y-1/2)(rz)}\Big)\,F_a^S(x,y;t)\,dy + O(r)\ \text{terms}\\
&= \bar{u}(p',s')\hat{z}u(p,s)\int\limits_{-1}^1 dx \int\limits_{-1+|x|}^{1-|x|}\mathrm{e}^{-ix(Pz)-i\alpha(rz)/2}\,\tilde{f}_a^S(x,\alpha\,;t)\,d\alpha + O(r)\ .
\end{aligned} \tag{17}$$

In the second and third lines here we have used the fact that positive-x and negative-x parts in this case are described by the same untilded function

$$F_a^S(x,y;t)|_{x\neq 0} = F_a(x,y;t) + F_{\bar{a}}(x,y;t).$$

The α-DDs $\tilde{f}_a^S(x,\alpha\,;\,t)$ are even functions of α and, according to Eq. (17), odd functions of x:

$$\tilde{f}_a^S(x,\alpha;t) = \{f_a(|x|,|\alpha|;t) + f_{\bar{a}}(|x|,|\alpha|;t)\}\,\mathrm{sign}(x) + f_M^S(x,\alpha;t)\ . \tag{18}$$

Finally, the valence quark functions $\tilde{f}_a^V(x,\alpha\,;\,t)$ related to the operators

$$\mathcal{O}_a^V\left(-\frac{z}{2},\frac{z}{2}\right) = \frac{1}{2}\left[\bar{\psi}_a\left(-\frac{z}{2}\right)\hat{z}E\left(-\frac{z}{2},\frac{z}{2};A\right)\psi_a\left(\frac{z}{2}\right) + \{z\to -z\}\right]$$

are even functions of both α and x:

$$\tilde{f}_a^V(x,\alpha;t) = f_a(|x|,|\alpha|;t) - f_{\bar{a}}(|x|,|\alpha|;t) + f_M^V(x,\alpha;t)\,. \tag{19}$$

3. Models for double and skewed distributions

The reduction formulas and interpretation of the x-variable as the fraction of p (or P) momentum suggest that the profile of $F(x,y)$ (or $f(x,\alpha)$) in x-direction is basically determined by the shape of $f(x)$. On the other hand, the profile in y (or α) direction characterizes the spread of the parton momentum induced by the momentum transfer r. In particular, since the α-DDs $\tilde{f}(x,\alpha)$ are even functions of α, it make sense to write

$$\tilde{f}(x,\alpha) = h(x,\alpha)\,\tilde{f}(x)\,, \tag{20}$$

where $h(x,\alpha)$ is an even function of α normalized by

$$\int\limits_{-1+|x|}^{1-|x|} h(x,\alpha)\,d\alpha \;= 1. \tag{21}$$

We may expect that the α-profile of $h(x,\alpha)$ is similar to that of a symmetric distribution amplitude (DA) $\varphi(\alpha)$. Since $|\alpha| \le 1-|x|$, to get a more complete analogy with DA's, it makes sense to rescale α as $\alpha = (1-|x|)\beta$ introducing the variable β with x-independent limits: $-1 \le \beta \le 1$. The simplest model is to assume that the profile in the β-direction is a universal function $g(\beta)$ for all x. Possible simple choices for $g(\beta)$ may be $\delta(\beta)$ (no spread in β-direction), $\frac{3}{4}(1-\beta^2)$ (characteristic shape for asymptotic limit of nonsinglet quark distribution amplitudes), $\frac{15}{16}(1-\beta^2)^2$ (asymptotic shape of gluon distribution amplitudes), *etc.* In the variables x,α, this gives

$$h^{(\infty)}(x,\alpha) = \delta(\alpha)\;\;,\;\; h^{(1)}(x,\alpha) = \frac{3}{4}\frac{(1-|x|)^2-\alpha^2}{(1-|x|)^3}\;\;,$$
$$h^{(2)}(x,\alpha) = \frac{15}{16}\frac{[(1-|x|)^2-\alpha^2]^2}{(1-|x|)^5}\;\;. \tag{22}$$

These models can be treated as specific cases of the general profile function

$$h^{(b)}(x,\alpha) = \frac{\Gamma(2b+2)}{2^{2b+1}\Gamma^2(b+1)}\frac{[(1-|x|)^2-\alpha^2]^b}{(1-|x|)^{2b+1}}\,, \tag{23}$$

whose width is governed by the parameter b.

The coefficient of proportionality $\zeta = r^+/p^+$ (or $\xi = r^+/2P^+$) between the plus components of the momentum transfer and initial (or average) momentum specifies the *skewedness* of the matrix elements. The characteristic feature implied by representations for double distributions [see, *e.g.*, Eq. (2)] is the absence of the ζ-dependence in the DDs $F(x,y)$ and ξ-dependence in

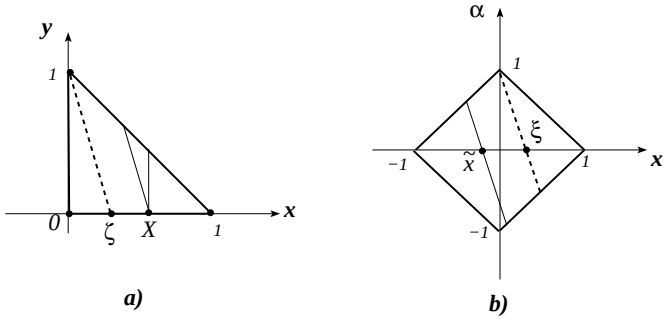

Fig. 4. Integration lines for integrals relating SPDs and DDs.

$f(x,\alpha)$. An alternative way to parametrize nonforward matrix elements of light-cone operators is to use ζ (or ξ) and the *total* momentum fractions $X \equiv x + y\zeta$ (or $\tilde{x} \equiv x + \xi\alpha$) as independent variables. Integrating each particular double distribution over y gives the nonforward parton distributions

$$\mathcal{F}^i_\zeta(X) = \int\limits_0^1 dx \int\limits_0^{1-x} \delta(x+\zeta y - X)\, F_i(x,y)\, dy$$

$$= \theta(X \geq \zeta) \int\limits_0^{\bar{X}/\bar{\zeta}} F_i(X - y\zeta, y)\, dy + \theta(X \leq \zeta) \int\limits_0^{X/\zeta} F_i(X - y\zeta, y)\, dy\,, \quad (24)$$

where $\bar{\zeta} \equiv 1 - \zeta$. The two components of NFPDs correspond to positive ($X > \zeta$) and negative ($X < \zeta$) values of the fraction $X' \equiv X - \zeta$ associated with the "returning" parton. As explained in Refs. [9, 11], the second component can be interpreted as the probability amplitude for the initial hadron with momentum p to split into the final hadron with momentum $(1-\zeta)p$ and the two-parton state with total momentum $r = \zeta p$ shared by the partons in fractions Yr and $(1-Y)r$, where $Y = X/\zeta$.

The relation between "untilded" NFPDs and DDs can be illustrated on the "DD-life triangle" defined by $0 \leq x, y, x+y \leq 1$ (see Fig. 4a). Specifically, to get $\mathcal{F}_\zeta(X)$, one should integrate $F(x,y)$ over y along a straight line $x = X - \zeta y$. Fixing some value of ζ, one deals with a set of parallel lines intersecting the x-axis at $x = X$. The upper limit of the y-integration is determined by intersection of this line either with the line $x + y = 1$ (this happens if $X > \zeta$) or with the y-axis (if $X < \zeta$). The line corresponding to $X = \zeta$ separates the triangle into two parts generating the two components of the nonforward parton distribution.

In a similar way, we can write the relation between OFPDs $H(\tilde{x},\xi;t)$ and the α-DDs $\tilde{f}(x,\alpha;t)$

$$H(\tilde{x},\xi;t)=\int\limits_{-1}^{1}dx\int\limits_{-1+|x|}^{1-|x|}\delta(x+\xi\alpha-\tilde{x})\,\tilde{f}(x,\alpha;t)\,d\alpha\,. \tag{25}$$

The delta-function in Eq. (25) specifies the line of integration in the $\{x,\alpha\}$ plane. For definiteness, we will assume below that ξ is positive.

Information contained in SPDs originates from two physically different sources: meson-exchange type contributions $\mathcal{F}^M_\zeta(X)$ coming from the singular $x=0$ parts of DDs and the functions $\mathcal{F}^a_\zeta(X)$, $\mathcal{F}^{\bar{a}}_\zeta(X)$ obtained by scanning the $x\neq 0$ parts of DDs $F^a(x,y)$, $F^{\bar{a}}(x,y)$. The support of exchange contributions is restricted to $0\le X\le\zeta$. Up to rescaling, the function $\mathcal{F}^M_\zeta(X)$ has the same shape for all ζ. For any nonvanishing X, these exchange terms become invisible in the forward limit $\zeta\to 0$. On the other hand, the support of functions $\mathcal{F}^a_\zeta(X)$, $\mathcal{F}^{\bar{a}}_\zeta(X)$ in general covers the whole $0\le X\le 1$ region. Furthermore, the forward limit of such SPDs as $\mathcal{F}^{a,\bar{a}}_\zeta(X)$ is rather well known from inclusive measurements. Hence, information contained in the usual (forward) densities $f^a(x)$, $f^{\bar{a}}(x)$ can be used to restrict the models for $\mathcal{F}^a_\zeta(X)$, $\mathcal{F}^{\bar{a}}_\zeta(X)$.

Let us consider SPDs constructed using simple models of DDs specified above. In particular, the model $f^{(\infty)}(x,\alpha)=\delta(\alpha)f(x)$ (equivalent to $F^{(\infty)}(x,y)=\delta(y-\bar{x}/2)f(x)$), gives the simplest model $H^{(\infty)}(\tilde{x},\xi;t=0)=f(x)$ in which OFPDs at $t=0$ have no ξ-dependence. For NFPDs this gives

$$\mathcal{F}^{(\infty)}_\zeta(X)=\frac{\theta(X\ge\zeta/2)}{1-\zeta/2}f\left(\frac{X-\zeta/2}{1-\zeta/2}\right), \tag{26}$$

i.e., NFPDs for non-zero ζ are obtained from the forward distribution $f(X)\equiv\mathcal{F}_{\zeta=0}(X)$ by shift and rescaling.

In the case of the $b=1$ and $b=2$ models, simple analytic results can be obtained only for some explicit forms of $f(x)$. For the "valence quark"-oriented ansatz $\tilde{f}^{(1)}(x,\alpha)$, the following choice of a normalized distribution

$$f^{(1)}(x)=\frac{\Gamma(5-a)}{6\,\Gamma(1-a)}\,x^{-a}(1-x)^3 \tag{27}$$

is both close to phenomenological quark distributions and produces a simple expression for the double distribution since the denominator $(1-x)^3$ factor in Eq. (22) is cancelled. As a result, the integral in Eq. (25) is easily performed

and we get

$$H^1_V(\tilde{x},\xi)|_{|\tilde{x}|\geq\xi} = \frac{1}{\xi^3}\left(1-\frac{a}{4}\right)\left\{\left[(2-a)\xi(1-\tilde{x})(x_1^{2-a}+x_2^{2-a})\right.\right.$$
$$\left.\left.+(\xi^2-\tilde{x})(x_1^{2-a}-x_2^{2-a})\right]\theta(\tilde{x})+(\tilde{x}\to-\tilde{x})\right\} \qquad (28)$$

for $|\tilde{x}|\geq\xi$ and

$$H^1_V(\tilde{x},\xi)|_{|\tilde{x}|\leq\xi} = \frac{1}{\xi^3}\left(1-\frac{a}{4}\right)\left\{x_1^{2-a}[(2-a)\xi(1-\tilde{x})+(\xi^2-x)]\right.$$
$$\left.+(\tilde{x}\to-\tilde{x})\right\} \qquad (29)$$

in the middle $-\xi \leq \tilde{x} \leq \xi$ region. We use here the notation $x_1 = (\tilde{x}+\xi)/(1+\xi)$ and $x_2 = (\tilde{x}-\xi)/(1-\xi)$ [23]. To extend these expressions onto negative values of ξ, one should substitute ξ by $|\xi|$. One can check, however, that no odd powers of $|\xi|$ would appear in the $\tilde{x}^N$ moments of $H^{1V}(\tilde{x},\xi)$. Furthermore, these expressions are explicitly non-analytic for $x=\pm\xi$. This is true even if a is integer. Discontinuity at $x=\pm\xi$, however, appears only in the second derivative of $H^{1V}(\tilde{x},\xi)$, *i.e.*, the model curves for $H^{1V}(\tilde{x},\xi)$ look very smooth (see Fig. 5). The explicit expressions for NFPDs in this model were given in Ref. [17]. The relevant curves are also shown in Fig. 5.

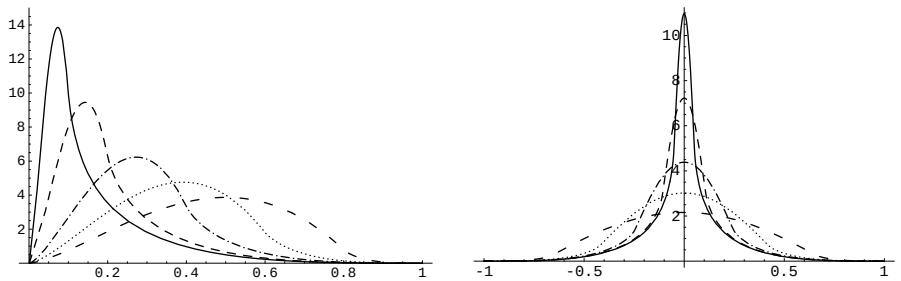

Fig. 5. Valence quark distributions: untilded NFPDs $F^q_\zeta(x)$ (left) and OFPDs $H^1_V(\tilde{x},\xi)$ (right) with $a=0.5$ for several values of ζ, namely, 0.1, 0.2, 0.4, 0.6, 0.8 and corresponding values of $\xi=\zeta/(2-\zeta)$. Lower curves correspond to larger values of ζ.

For $a=0$, the $x>\xi$ part of OFPD has the same x-dependence as its forward limit, differing from it by an overall ξ-dependent factor only:

$$H^{1V}(\tilde{x},\xi)|_{a=0} = 4\,\frac{(1-|\tilde{x}|)^3}{(1-\xi^2)^2}\,\theta(|\tilde{x}|\geq\xi) + 2\,\frac{\xi+2-3\frac{\tilde{x}^2}{\xi}}{(1+\xi)^2}\,\theta(|\tilde{x}|\leq\xi)\,. \qquad (30)$$

The $(1-|\tilde{x}|)^3$ behaviour can be trivially continued into the $|\tilde{x}|<\xi$ region. However, the actual behaviour of $H^{1V}(\tilde{x},\xi)|_{a=0}$ in this region is given by a different function. In other words, $H^{1V}(\tilde{x},\xi)|_{a=0}$ can be represented as a sum of a function analytic at border points and a contribution whose support is restricted by $|\tilde{x}|\leq\xi$. It should be emphasized that despite its DA-like appearance, this contribution should not be treated as an exchange-type term. It is generated by regular $x\neq 0$ part of DD, and, unlike $\varphi(\tilde{x}/\xi)/\xi$ functions changes its shape with ξ and becomes very small for small ξ.

For the singlet quark distribution, the α-DDs $\tilde{f}^S(x,\alpha)$ should be odd functions of x. Still, we can use the model like (27) for the $x>0$ part, but take $\tilde{f}^S(x,\alpha)|_{x\neq 0}=A\,f^{(1)}(|x|,\alpha)\,\mathrm{sign}(x)$. Note, that the integral (25) producing $H^S(\tilde{x},\xi)$ in the $|\tilde{x}|\leq\xi$ region would diverge for $\alpha\to\tilde{x}/\xi$ if $a\geq 1$, which is the usual case for standard parametrizations of singlet quark distributions for sufficiently large Q^2. However, due to the antisymmetry of $\tilde{f}^S(x,\alpha)$ wrt $x\to -x$ and its symmetry wrt $\alpha\to-\alpha$, the singularity at $\alpha=\tilde{x}/\xi$ can be integrated using the principal value prescription which in this case produces the $x\to -x$ antisymmetric version of Eqs.(28) and (29). For $a=0$, its middle part reduces to

$$H^{1S}(\tilde{x},\xi)|_{|\tilde{x}|\leq\xi,a=0}=2x\,\frac{3\xi^2-2x^2\xi-x^2}{\xi^3(1+\xi)^2}\,. \tag{31}$$

The shape of singlet SPDs in this model is shown in Fig. 6

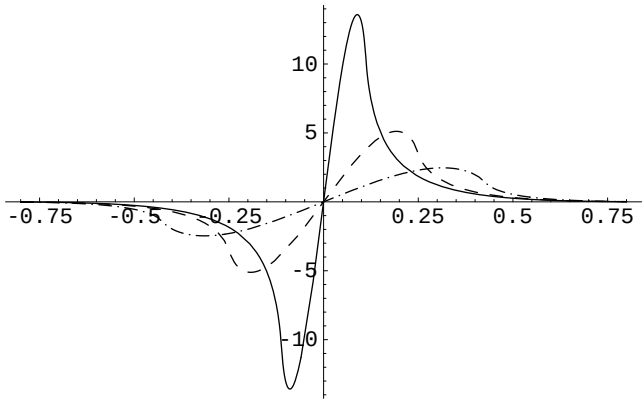

Fig. 6. Singlet quark distribution $H^1_S(\tilde{x},\xi)$ for several ξ values 0.1, 0.25, 0.4. Lower curves correspond to larger values of ξ. Forward distribution is modelled by $(1-x)^3/x$.

4. SPDs and deeply virtual Compton scattering

In the lowest order, the DVCS amplitude $T^{\mu\nu}(p,q,q')$ is given by two handbag diagrams. In particular, the invariant amplitude containing the $\mathcal{F}$ functions is given by

$$T_F(p,q,q') = \sum_a e_a^2 \int\limits_0^1 \left[\frac{1}{X-\zeta+i\varepsilon} + \frac{1}{X-i\varepsilon}\right] \mathcal{F}_\zeta^{a+\bar a}(X;t)\, dX\,. \qquad (32)$$

An important feature of the DVCS amplitude is that for large Q^2 and fixed t it depends only on the ratio $Q^2/2(pq) \equiv x_{Bj} = \zeta$: DVCS is an *exclusive* process exhibiting the Bjorken scaling. Note that the imaginary part of the DVCS amplitude is proportional to $\mathcal{F}_\zeta^{a+\bar a}(\zeta;t)$. In this function, the parameter ζ appears twice: first as the skewedness of the process and then as the fraction $X=\zeta$ at which the imaginary part is generated.

One may ask which Q^2 are large enough to ensure the dominance of the lowest-twist handbag contribution. In DIS, approximate Bjorken scaling starts at $Q^2 \sim 2\,\mathrm{GeV}^2$. Another example is given by the exclusive process $\gamma(q_1)\gamma^*(q_2) \to \pi^0$ studied at e^+e^- colliders. If one of the photons is highly virtual $q_1^2 = -Q^2$ while another is (almost) real $q_2^2 \sim 0$, the process is kinematically similar to DVCS. In the leading order, the $F_{\gamma\gamma^*\pi^0}(Q^2)$ transition form factor is given by a handbag diagram again. The recent measurements by CLEO [24] show that the pQCD prediction $F_{\gamma\gamma^*\pi^0}(Q^2) \sim 1/Q^2$ again works starting from $Q^2 \sim 2\,\mathrm{GeV}^2$. The $\gamma\gamma^*\pi^0$ vertex (for a virtual pion) can be also measured on a fixed-target machine like CEBAF in which case it is just a part of the DVCS amplitude corresponding to the 4th skewed distribution $\mathcal{P}_\zeta(X,t)$ (which is related to the pseudoscalar form factor $G_P(t)$ of the nucleon). Hence, CLEO data give an evidence that DVCS may be handbag-dominated for Q^2 as low as $2\,\mathrm{GeV}^2$.

The main problem for studying DVCS is the contamination by the Bethe–Heitler process in which the final photon is emitted from the initial or final electron. The Bethe–Heitler amplitude is enhanced at small t. On the other hand, the virtual photon flux for fixed Q^2 and x_{Bj} increases when the electron beam energy increases. Hence, the energy upgrade would make the DVCS studies at Jefferson Lab more feasible. Experimental aspects of virtual Compton scattering studies at Jefferson Lab are discussed in Refs. [25].

The skewed parton distributions can be also measured in hard meson electroproduction processes [11,12,22,25]. The leading-twist pQCD contribution in this case involves a one-gluon exchange, which means that the hard subprocess is suppressed by $\alpha_s/\pi \sim 0.1$ factor. The competing soft mechanism corresponds to a triple overlap of hadronic wave functions and has a relative suppression M^2/Q^2 by a power of Q^2, with $M^2 \sim 1$ GeV^2 being a

characteristic hadronic scale. Hence, to clearly see the one-gluon-exchange signal one needs Q^2 above $10\,\mathrm{GeV}^2$. Numerical pQCD-based estimates and comparison of DVCS and hard meson electroprodution cross sections can be found in Ref. [25].

5. SPD enhancement factor

The imaginary part of hard exclusive meson electroproduction amplitude is determined by the skewed distributions at the border point. For this reason, the magnitude of $\mathcal{F}_\zeta(\zeta)$ [or $H(\xi,\xi)$] and its relation to the forward densities $f(x)$ has a practical interest. This example also gives a possibility to study the sensititivity of the results to the choice of the profile function. Assuming the infinitely narrow weight $\rho(\alpha)=\delta(\alpha)$, we have $\mathcal{F}_\zeta(X)=f(X-\zeta/2)+\ldots$ and $H(x,\xi)=f(x)$. Hence, both $\mathcal{F}_\zeta(\zeta)$ and $H(\xi,\xi)$ are given by $f(x_{Bj}/2)$ since $\zeta=x_{Bj}$ and $\xi=x_{Bj}/2+\ldots$. Since the argument of $f(x)$ is twice smaller than in deep inelastic scattering, this results in an enhancement factor. In particular, if $f(x)\sim x^{-a}$ for small x, the ratio $\mathcal{R}(\zeta)\equiv\mathcal{F}_\zeta(\zeta)/f(\zeta)$ is 2^a. The use of a wider profile function $\rho(\alpha)$ produces further enhancement. For example, taking the normalized profile function

$$\rho_b(\alpha)\equiv\frac{\Gamma\left(b+\frac{3}{2}\right)}{\Gamma\left(\frac{1}{2}\right)\Gamma(b+1)}(1-\alpha^2)^b=\frac{\Gamma(2b+2)}{2^{2b+1}\Gamma^2(b+1)}(1-\alpha^2)^b \tag{33}$$

and $f(x)\sim x^{-a}$ we get

$$\mathcal{R}^{(b)}(\zeta)\equiv\frac{\mathcal{F}_\zeta^{(b)}(\zeta)}{f(\zeta)}=\frac{\Gamma(2b+2)\Gamma(b-a+1)}{\Gamma(2b-a+2)\Gamma(b+1)} \tag{34}$$

which is larger than 2^a for any finite b and $0<a<2$. The 2^a enhancement appears as the $b\to\infty$ limit of Eq. (33). For small integer b, Eq. (33) reduces to simple formulas obtained in Refs. [17,18]. For $b=1$, we have

$$\frac{\mathcal{F}_\zeta^{(b=1)}(\zeta)}{f(\zeta)}=\frac{1}{\left(1-\frac{a}{2}\right)\left(1-\frac{a}{3}\right)}\,, \tag{35}$$

which gives the factor of 3 for the enhancement if $a=1$. For $b=2$, the ratio (33) becomes

$$\frac{\mathcal{F}_\zeta^{(b=2)}(\zeta)}{f(\zeta)}=\frac{1}{\left(1-\frac{a}{3}\right)\left(1-\frac{a}{4}\right)\left(1-\frac{a}{5}\right)}\,, \tag{36}$$

producing a smaller enhancement factor $5/2$ for $a=1$. Calculating the enhancement factors, one should remember that the gluon SPD $\mathcal{F}_\zeta(X)$ reduces

to $Xf_g(X)$ in the $\zeta = 0$ limit. Hence, to get the enhancement factor corresponding to the $f_g(x) \sim x^{-\lambda}$ small-x behavior of the forward gluon density, one should take $a = \lambda - 1$ in Eq. (33), *i.e.*, despite the fact that the $1/x$ behavior of the singlet quark distribution gives the factor of 3 for the $\mathcal{R}^{(1)}(\zeta)$ ratio, the same shape of the gluon distribution results in no enhancement.

Due to evolution, the effective parameter a characterizing the small-x behavior of the forward distribution is an increasing function of Q^2. As a result, for fixed b, the $\mathcal{R}^{(b)}(\zeta)$ ratio increases with Q^2. In general, the profile of $\tilde{f}(\tilde{x}, \alpha)$ in the α-direction is also affected by the pQCD evolution. In particular, in Ref. [17] it was shown that if one takes an ansatz corresponding to an extremely asymmetric profile function $\rho(\alpha) \sim \delta(1+\alpha)$, the shift of the profile function to a more symmetric shape is clearly visible in the evolution of the relevant SPD. Recently, it was demonstrated [26,27] that evolution to sufficiently large Q^2 enforces a direct relation $b = a$ between the parameter a characterizing the small-x behavior of DDs and the parameter b governing the shape of their α profile. This gives

$$\mathcal{R}^{(b=a)}(\zeta) = \frac{\Gamma(2a+2)}{\Gamma(a+2)\Gamma(a+1)} \tag{37}$$

for the $\mathcal{R}(\zeta)$ ratio. For $a = 1$, *e.g.*, the SPD enhancement factor in this case equals 3.

6. Compton scattering

6.1. General Compton amplitude

The Compton scattering in its various versions provides a unique tool for studying hadronic structure. The Compton amplitude probes the hadrons through a coupling of two electromagnetic currents and in this aspect it can be considered as a generalization of hadronic form factors. In QCD, the photons interact with the quarks of a hadron through a vertex which, in the lowest approximation, has a pointlike structure. However, in the soft regime, strong interactions produce large corrections uncalculable within the perturbative QCD framework. To take advantage of the basic pointlike structure of the photon–quark coupling and the asymptotic freedom feature of QCD, one should choose a specific kinematics in which the behavior of the relevant amplitude is dominated by short (or, being more precise, lightlike) distances. The general feature of all such types of kinematics is the presence of a large momentum transfer. For Compton amplitudes, there are several situations when large momentum transfer induces dominance of configurations involving lightlike distances:

i) both photons are far off-shell and have equal spacelike virtuality: virtual forward Compton amplitude, its imaginary part determines structure functions of deep inelastic scattering (DIS);

ii) initial photon is highly virtual, the final one is real and the momentum transfer to the hadron is small: deeply virtual Compton scattering (DVCS) amplitude;

iii) both photons are real but the momentum transfer is large: wide-angle Compton scattering (WACS) amplitude.

Our main statement made in Ref. [21] is that, at accessible momentum transfers $|t| < 10$ GeV^2, the WACS amplitude is dominated by handbag diagrams, just like in DIS and DVCS. In the most general case, the nonperturbative part of the handbag contribution is described by double distributions (DDs) $F(x,y;t), G(x,y;t)$, *etc.*, which can be related to the usual parton densities $f(x)$, $\Delta f(x)$ and nucleon form factors like $F_1(t), G_A(t)$. Among the arguments of DDs, x is the fraction of the initial hadron momentum carried by the active parton and y is the fraction of the momentum transfer r. The description of WACS amplitude simplifies when one can neglect the y-dependence of the hard part and integrate out the y-dependence of the double distributions. In that case, the long-distance dynamics is described by nonforward parton densities (NDs) $\mathcal{F}(x;t), \mathcal{G}(x;t)$, *etc.* The latter can be interpreted as the usual parton densities $f(x)$ supplemented by a form factor type t-dependence. We proposed in [21] a simple model for the relevant NDs which both satisfies the relation between $\mathcal{F}(x;t)$ and usual parton densities $f(x)$ and produces a good description of the $F_1(t)$ form factor up to $t \sim -10$ GeV^2. We have used this model to calculate the WACS amplitude and obtained the results which are rather close to existing data.

6.2. Deep inelastic scattering

The forward virtual Compton amplitude whose imaginary part gives structure functions of deep inelastic scattering (see, *e.g.*, [1]) is the classic example of a light cone dominated Compton amplitude. In this case, the "final" photon has momentum $q' = q$ coinciding with that of the initial one. The momenta p, p' of the initial and final hadrons also coincide. The total cm energy of the photon–hadron system $s = (p+q)^2$ should be above resonance region, and the Bjorken ratio $x_{Bj} = Q^2/2(pq)$ is finite. The light cone dominance is secured by high virtuality of the photons: $-q^2 \equiv Q^2 > 1$ GeV^2. In the large-Q^2 limit, the leading contribution in the lowest α_s order is given by handbag diagrams in which the perturbatively calculable hard quark propagator is convoluted with parton distribution

functions $f_a(x)$ $(a = u, d, s, \ldots)$ which describe/parametrize nonperturbative information about hadronic structure.

6.3. Deeply virtual Compton scattering

The condition that both photons are highly virtual may be relaxed by taking a real photon in the final state. Keeping the momentum transfer $t \equiv (p - p')^2$ to the hadron as small as possible, one arrives at kinematics of the deeply virtual Compton scattering (DVCS) the importance of which was recently emphasized by Ji [8] (see also [9]). Having large virtuality Q^2 of the initial photon is sufficient to guarantee that in the Bjorken limit the leading power contributions in $1/Q^2$ are generated by the strongest light cone singularities [8,11,28,29], with the handbag diagrams being the starting point of the α_s expansion. The most important contribution to the DVCS amplitude is given by a convolution of a hard quark propagator and a nonperturbative function describing long-distance dynamics, which in the most general case is given by double distributions (DDs) $F(x, y; t), G(x, y; t), \ldots$ [9,11].

In the DVCS kinematics, $|t|$ is assumed to be small compared to Q^2, and for this reason the t- and m_p^2-dependence of the short-distance amplitude in Refs. [8,9,11,23] was neglected[1]. This is equivalent to approximating the active parton momentum k by its plus component alone: $k \to xp^+ + yr^+$.

7. Modeling NDs

Our final goal in the present paper is to get an estimate of the handbag contributions for the large-t real Compton scattering. Since the initial photon in that case is also real: $Q^2 = 0$ (and hence $x_{Bj} = 0$), it is natural to expect that the nonperturbative functions which appear in WACS correspond to the $\zeta = 0$ limit of the skewed parton distributions[2] $\mathcal{F}^a_\zeta(x; t)$. It is easy to see from Eq. (10) that in this limit the SPDs reduce to the nonforward parton densities $\mathcal{F}^a(x; t)$ introduced above:

$$\mathcal{F}^a_{\zeta=0}(x; t) = \mathcal{F}^a(x; t)\,. \tag{38}$$

Note that NDs depend on "only two" variables x and t, with this dependence constrained by reduction formulas (11),(12). Furthermore, it is possible to give an interpretation of nonforward densities in terms of the light-cone wave functions.

[1] One should not think that such a dependence is necessarily a higher twist effect: the lowest twist contribution has a calculable dependence on t and m_p^2 analogous to the Nachtmann–Georgi–Politzer $O(m_p^2/Q^2)$ target mass corrections in DIS [30,31].

[2] Provided that one can neglect the t-dependence of the hard part.

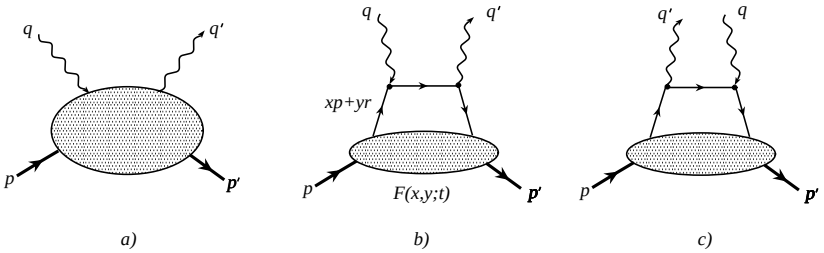

Fig. 7. a) General Compton amplitude; b) s-channel handbag diagram; c) u-channel handbag diagram.

Consider for simplicity a two-body bound state whose lowest Fock component is described by a light cone wave function $\Psi(x, k_\perp)$. Choosing a frame where the momentum transfer r is purely transverse $r = r_\perp$, we can write the two-body contribution into the form factor as [32]

$$F^{(tb)}(t) = \int_0^1 dx \int \Psi^*(x, k_\perp + \bar{x} r_\perp)\, \Psi(x, k_\perp)\, \frac{d^2 k_\perp}{16\pi^3}\,, \tag{39}$$

where $\bar{x} \equiv 1 - x$. Comparing this expression with the reduction formula (11), we conclude that

$$\mathcal{F}^{(tb)}(x, t) = \int \Psi^*(x, k_\perp + \bar{x} r_\perp)\, \Psi(x, k_\perp)\, \frac{d^2 k_\perp}{16\pi^3} \tag{40}$$

is the two-body contribution into the nonforward parton density $\mathcal{F}(x, t)$.

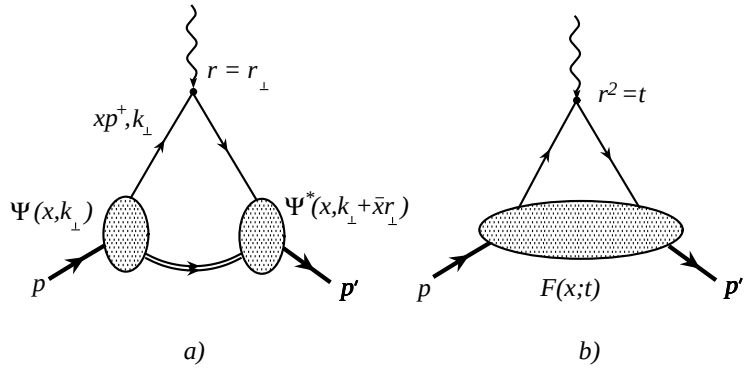

Fig. 8. a) Structure of the effective two-body contribution to form factor in the light cone formalism. b) Form factor as an x-integral of nonforward parton densities.

Assuming a Gaussian dependence on the transverse momentum $k_\perp$ (*cf.* [32])

$$\Psi(x,k_\perp) = \Phi(x)\mathrm{e}^{-k_\perp^2/2x\bar{x}\lambda^2}\,, \tag{41}$$

we get

$$\mathcal{F}^{(tb)}(x,t) = f^{(tb)}(x)\mathrm{e}^{\bar{x}t/4x\lambda^2}\,, \tag{42}$$

where

$$f^{(tb)}(x) = \frac{x\bar{x}\lambda^2}{16\pi^2}\,\Phi^2(x) = \mathcal{F}^{(tb)}(x,t=0) \tag{43}$$

is the two-body part of the relevant parton density. Within the light-cone approach, to get the total result for either usual $f(x)$ or nonforward parton densities $\mathcal{F}(x,t)$, one should add the contributions due to higher Fock components. By no means these contributions are small, *e.g.*, the valence $\bar{d}u$ contribution into the normalization of the π^+ form factor at $t=0$ is less than 25% [32]. In the absence of a formalism providing explicit expressions for an infinite tower of light-cone wave functions we choose to treat Eq. (42) as a guide for fixing interplay between the t and x dependences of NDs and propose to model them by

$$\mathcal{F}^a(x,t) = f_a(x)\mathrm{e}^{\bar{x}t/4x\lambda^2} = \frac{f_a(x)}{\pi x\bar{x}\lambda^2}\int \mathrm{e}^{-(k_\perp^2+(k_\perp+\bar{x}r_\perp)^2)/2x\bar{x}\lambda^2}d^2k_\perp\,. \tag{44}$$

The functions $f_a(x)$ here are the usual parton densities assumed to be taken from existing parametrizations like GRV, MRS, CTEQ, *etc.* In the $t=0$ limit (recall that t is negative) this model, by construction, satisfies the first of reduction formulas (11). Within the Gaussian ansatz (44), the basic scale λ specifies the average transverse momentum carried by the quarks. In particular, for valence quarks

$$\langle k_\perp^2\rangle^a = \frac{\lambda^2}{N_a}\int\limits_0^1 x\bar{x}f_a^{\mathrm{val}}(x)\,dx\,, \tag{45}$$

where $N_u=2, N_d=1$ are the numbers of the valence a-quarks in the proton.

To fix the magnitude of λ, we use the second reduction formula in (11) relating $\mathcal{F}^a(x,t)$'s to the $F_1(t)$ form factor. To this end, we take the following simple expressions for the valence distributions

$$f_u^{\mathrm{val}}(x) = 1.89\,x^{-0.4}(1-x)^{3.5}(1+6x)\,, \tag{46}$$

$$f_d^{\mathrm{val}}(x) = 0.54\,x^{-0.6}(1-x)^{4.2}(1+8x)\,. \tag{47}$$

They closely reproduce the relevant curves given by the GRV parametrization [33] at a low normalization point $Q^2 \sim 1$ GeV^2. The best agreement between our model

$$F_1^{\rm soft}(t) = \int\limits_0^1 \Big[e_u\, f_u^{\rm val}(x) + e_d\, f_d^{\rm val}(x) \Big]\, {\rm e}^{\bar{x}t/4x\lambda^2} dx \tag{48}$$

and experimental data [34] in the moderately large t region $1\ {\rm GeV}^2 < |t| < 10\ {\rm GeV}^2$ is reached for $\lambda^2 = 0.7\ {\rm GeV}^2$ (see Fig. 9). This value gives a reasonable magnitude

$$\langle k_\perp^2 \rangle^u = (290\,{\rm MeV})^2\,, \qquad \langle k_\perp^2 \rangle^d = (250\,{\rm MeV})^2 \tag{49}$$

for the average transverse momentum of the valence u and d quarks in the proton.

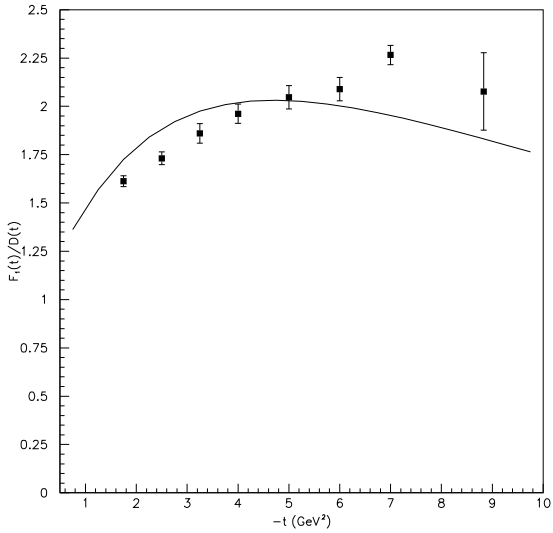

Fig. 9. Ratio $F_1^p(t)/D(t)$ of the $F_1^p(t)$ form factor to the dipole fit $D(t) = 1/(1 - t/0.71\,{\rm GeV}^2)^2$. Curve is based on Eq. (47) with $\lambda^2 = 0.7\,{\rm GeV}^2$. Experimental data are taken from Ref. [34].

Similarly, building a model for the parton helicity sensitive NDs $\mathcal{G}^a(x,t)$ one can take their $t = 0$ shape from existing parametrizations for spin-dependent parton distributions $\Delta f_a(x)$ and then fix the relevant λ parameter by fitting the $G_A(t)$ form factor. The case of hadron spin-flip distributions $\mathcal{K}^a(x,t)$ and $\mathcal{P}^a(x;t)$ is more complicated since the distributions $k_a(x)$, $p_a(x)$ are unknown.

At $t = 0$, our model by construction gives a correct normalization $F_1^p(t = 0) = 1$ for the form factor. However, if one would try to find the derivative $(d/dt)F_1^p(t)$ at $t = 0$ by expanding the exponential $\exp[\bar{x}t/x\lambda^2]$ into the Taylor series under the integral (48), one would get a divergent expression. An analogous problem is well known in applications of QCD sum rules to form factors at small t [35–38]. The divergence is related to the long-distance propagation of massless quarks in the t-channel. Formally, this is revealed by singularities starting at $t = 0$. However, $F_1^p(t)$ should not have singularities for timelike t up to $4m_\pi^2$, with the ρ-meson peak at $t = m_\rho^2 \sim 0.6\,\mathrm{GeV}^2$ being the most prominent feature of the t-channel spectrum. Technically, the singularities of the original expression are singled out into the bilocal correlators [39] which are substituted by their realistic version with correct spectral properties (usually the simplest model with ρ and ρ' terms is used). An important point is that such a modification is needed only when one calculates form factors in the small-t region: for $-t > 1\,\mathrm{GeV}^2$, the correction terms should vanish faster than any power of $1/t$ [37]. In our case, the maximum deviation of the curve for $F_1^p(t)$ given by Eq. (48) from the experimental data in the small-t region $-t < 1\,\mathrm{GeV}^2$ is 15%. Hence, if one is willing to tolerate such an inaccuracy, one can use our model starting with $t = 0$.

Our curve is within 5% from the data points [34] for $1\,\mathrm{GeV}^2 < -t < 6$ GeV^2 and does not deviate from them by more than 10% up to 9 GeV^2. Modeling the t-dependence by a more complicated formula (*e.g.*, assuming a slower decrease at large t, and/or choosing different λ's for u and d quarks and/or splitting NDs into several components with different λ's, *etc.*, see Ref. [40] for an example of such an attempt) or changing the shape of parton densities $f_a(x)$ one can improve the quality of the fit and extend agreement with the data to higher t. Such a fine-tuning is not our goal here. We just want to emphasize that a reasonable description of the $F_1(t)$ data in a wide region $1\ \mathrm{GeV}^2 < |t| < 10\ \mathrm{GeV}^2$ was obtained by fixing just a single parameter λ reflecting the proton size. Moreover, we could fix λ from the requirement that $\langle k_\perp^2 \rangle \sim (300\,\mathrm{MeV})^2$ and present our curve for $F_1(t)$ as a successful prediction of the model. We interpret this success as an evidence that the model correctly catches the gross features of the underlying physics.

Since our model implies a Gaussian dependence on the transverse momentum, it includes only what is usually referred to as an overlap of soft wave functions. It completely neglects effects due to hard pQCD gluon exchanges generating the power-law $O((\alpha_s/\pi)^2/t^2)$ tail of the nonforward densities at large t. It is worth pointing out here that though we take nonforward densities $\mathcal{F}^a(x,t)$ with an exponential dependence on t, the $F_1(t)$ form factor in our model has a power-law asymptotics $F_1^{\mathrm{soft}}(t) \sim (-4\lambda^2/t)^{n+1}$ dictated by the $(1-x)^n$ behavior of the parton densities for x close to 1. This con-

nection arises because the integral (48) over x is dominated at large t by the region $\bar{x} \sim 4\lambda^2/|t|$. In other words, the large-t behavior of $F_1(t)$ in our model is governed by the Feynman mechanism [1]. One should realize, however, that the relevant scale $4\lambda^2 = 2.8$ GeV^2 is rather large. For this reason, when $|t| < 10$ GeV^2, it is premature to rely on asymptotic estimates for the soft contribution. Indeed, with $n = 3.5$, the asymptotic estimate is $F_1^{\rm soft}(t) \sim t^{-4.5}$, in an apparent contradiction with the ability of our curve to follow the dipole behavior. The resolution of this paradox is very simple: the maxima of nonforward densities $\mathcal{F}^a(x,t)$ for $|t| < 10$ GeV^2 are at rather low x-values $x < 0.5$. Hence, the x-integrals producing $F_1^{\rm soft}(t)$ are not dominated by the $x \sim 1$ region yet and the asymptotic estimates are not applicable: the functional dependence of $F_1^{\rm soft}(t)$ in our model is much more complicated than a simple power of $1/t$.

The fact that our model closely reproduces the experimentally observed dipole-like behavior of the proton form factor is a clear demonstration that such a behavior may have nothing to do with the quark counting rules $F_1^p(t) \sim 1/t^2$ [41, 42] valid for the asymptotic behavior of the hard gluon exchange contributions. Our explanation of the observed magnitude and the t-dependence of $F_1(t)$ by a purely soft contribution is in strong contrast with that of the hard pQCD approach to this problem.

8. Wide-angle Compton scattering

With both photons real, it is not sufficient to have large photon energy to ensure short-distance dominance: large-s, small-t region is strongly affected by Regge contributions. Hence, having large $|t| > 1\,$GeV^2 is a necessary condition for revealing short-distance dynamics.

The simplest contributions for the WACS amplitude are given by the s- and u-channel handbag diagrams Fig. 7b,c. The nonperturbative part in this case is given by the proton DDs which determine the t-dependence of the total contribution. Just like in the form factor case, the contribution dominating in the formal asymptotic limit $s, |t|, |u| \to \infty$, is given by diagrams corresponding to the pure SD regime, see Fig. 10a. The hard subraph then involves two hard gluon exchanges which results in a suppression factor $(\alpha_s/\pi)^2 \sim 1/100$ absent in the handbag term. The total contribution of all two-gluon exchnange contributions was calculated by Farrar and Zhang [43] and then recalculated by Kronfeld and Nižić [44]. A sufficiently large contribution is only obtained if one uses humpy DAs and $1/k^2$ propagators with no finite-size effects included. Even with such propagators, the WACS amplitude calculated with the asymptotic DA is negligibly small [45] compared to existing data. As argued in Ref. [21], the enhancements generated by the humpy DAs should not be taken at face value both for form factors and

wide-angle Compton scattering amplitudes. For these reasons, we ignore hard contributions to the WACS amplitude as negligibly small.

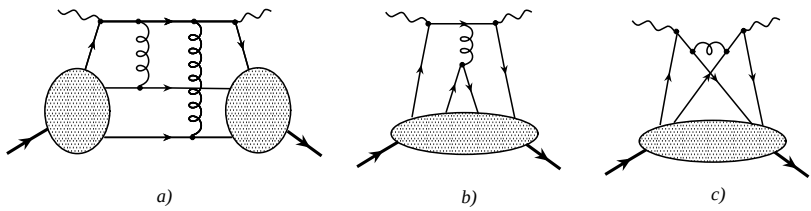

Fig. 10. Configurations involving double and single gluon exchange.

Another type of configurations containing hard gluon exchange is shown in Fig. 10b. There are also the diagrams with photons coupled to different quarks ("cat's ears", Fig. 10c). Such contributions have both higher order and higher twist. This brings in the α_s/π factor and an extra $1/s$ suppression. The latter is partially compensated by a slower fall-off of the four-quark DDs with t since only one valence quark should change its momentum.

For simplicity, we neglect all the suppressed terms and deal only with the handbag contributions Fig. 7b,c in which the highly virtual quark propagator connecting the photon vertices is convoluted with proton DDs parametrizing the overlap of soft wave functions. Since the basic scale $4\lambda^2$ characterizing the t-dependence of DDs in our model is 2.8 GeV^2, while existing data are all at momentum transfers t below 5 GeV^2, we deal with the region where the asymptotic estimate (Feynman mechanism) for the overlap contribution is not working yet. In the coordinate representation, the sum of two handbag contributions to the Compton amplitude can be written as

$$M^{\mu\nu}(p,p';q,q') = \sum_a e_a^2 \int \mathrm{e}^{-i(Qz)} \langle p'| \left(\bar\psi_a\left(\frac{z}{2}\right)\gamma^\mu S^c(z)\gamma^\nu \psi_a\left(-\frac{z}{2}\right)\right.$$
$$\left. +\bar\psi_a\left(-\frac{z}{2}\right)\gamma^\nu S^c(-z)\gamma^\mu \psi_a\left(\frac{z}{2}\right)\right)|p\rangle\, d^4z \qquad (50)$$

where $Q=(q+q')/2$ and $S^c(z) = i\hat z/2\pi^2(z^2)^2$ is the hard quark propagator (throughout, we use the "hat" notation $\hat z \equiv z_\alpha\gamma^\alpha$). The summation over the twist-0 longitudinal gluons adds the usual gauge link between the $\bar\psi$,ψ fields which we do not write down explicitly (gauge link disappears, *e.g.*, in the Fock–Schwinger gauge $z^\alpha A_\alpha(z)=0$). Because of the symmetry of the problem, it is convenient to use $P=(p+p')/2$ (*cf.* [8]) and $r=p-p'$ as the basic momenta. Applying the Fiertz transformation and introducing the

double distributions by

$$\langle p'|\bar\psi_a\left(-\frac{z}{2}\right)\hat z\psi_a\left(\frac{z}{2}\right)|p\rangle = \bar u(p')\hat z u(p)\int\limits_0^1 dx\int\limits_{-\bar x}^{\bar x}\Big[\mathrm{e}^{-i(kz)}f^a(x,\alpha;t)$$
$$-\mathrm{e}^{i(kz)}f^{\bar a}(x,\alpha;t)\Big]\,d\tilde y+\frac{1}{4m_p}\,\bar u(p')(\hat z\hat r-\hat r\hat z)u(p)$$
$$\times\int\limits_0^1 dx\int\limits_{-\bar x}^{\bar x}\Big[\mathrm{e}^{-i(kz)}k^a(x,\alpha;t)-\mathrm{e}^{i(kz)}k^{\bar a}(x,\alpha;t)\Big]\,d\alpha+O(z^2)\text{ terms}\quad(51)$$

(we use here the shorthand notation $k\equiv xP+\alpha r/2$) and similarly for the parton helicity sensitive operators

$$\langle p'|\bar\psi_a\left(-\frac{z}{2}\right)\hat z\gamma_5\psi_a\left(\frac{z}{2}\right)|p\rangle=\bar u(p')\hat z\gamma_5 u(p)\int\limits_0^1 dx\int\limits_{-\bar x}^{\bar x}\Big[\mathrm{e}^{-i(kz)}g^a(x,\alpha;t)$$
$$+\mathrm{e}^{i(kz)}g^{\bar a}(x,\alpha;t)\Big]\,d\alpha+\frac{(rz)}{m_p}\,\bar u(p')\gamma_5 u(p)$$
$$\times\int\limits_0^1 dx\int\limits_{-\bar x}^{\bar x}\Big[\mathrm{e}^{-i(kz)}p^a(x,\tilde y;t)+\mathrm{e}^{i(kz)}p^{\bar a}(x,\alpha;t)\Big]\,d\alpha+O(z^2)\text{ terms},\qquad(52)$$

we arrive at a leading-twist QCD parton picture with α-DDs serving as functions describing long-distance dynamics. The α-DDs $f^a(x,\alpha;t)$, *etc.*, are related to the original y-DDs $F^a(x,y;t)$ by the shift $y=(1-x+\alpha)/2$. Integrating $f(x,\alpha;t)$ over α one obtains the same nonforward densities $\mathcal{F}(x;t)$. The hard quark propagators for the s and u channel handbag diagrams in this picture look like

$$\frac{x\hat P+\alpha\frac{\hat r}{2}+\hat Q}{(xP+\alpha\frac{r}{2}+Q)^2}=\frac{x\hat P+\alpha\frac{\hat r}{2}+\hat Q}{x\tilde s-(\bar x^2-\alpha^2)\frac{t}{4}+x^2m_p^2}\qquad(53)$$

and

$$\frac{x\hat P+\alpha\frac{\hat r}{2}-\hat Q}{(xP+\alpha\frac{r}{2}-Q)^2}=\frac{x\hat P+\alpha\frac{\hat r}{2}-\hat Q}{x\tilde u-(\bar x^2-\alpha^2)\frac{t}{4}+x^2m_p^2},\qquad(54)$$

respectively. We denote $\tilde s=2(pq)=s-m^2$ and $\tilde u=-2(pq')=u-m^2$. Since α-DDs are even functions of α [22], the $\alpha\hat r$ terms in the numerators can be dropped. It is legitimate to keep $O(m_p^2)$ and $O(t)$ terms in the denominators: the dependence of hard propagators on target parameters m_p^2 and t can be

calculated exactly because of the effect analogous to the ξ-scaling in DIS [31] (see also [46]). Note that the t-correction to hard propagators disappears in the large-t limit dominated by the $x \sim 1$ integration. The t-corrections are the largest for $y = 0$. At this value and for $x = 1/2$ and $t = u$ (cm angle of 90°), the t-term in the denominator of the most important second propagator is only $1/8$ of the u term. This ratio increases to $1/3$ for $x = 1/3$. However, at nonzero α-values, the t-corrections are smaller. Hence, the t-corrections in the denominators of hard propagators can produce 10%–20% effects and should be included in a complete analysis. Here, we consider an approximation in which these terms are neglected and hard propagators are given by $\tilde{y}$-independent expressions $(x\hat{P} + \hat{Q})/x\tilde{s}$ and $(x\hat{P} + \hat{Q})/x\tilde{u}$. As a result, the α-integration acts only on the DDs $f(x, \alpha; t)$ and converts them into nonforward densities $\mathcal{F}(x, t)$. The latter would appear then through two types of integrals

$$\int\limits_0^1 \mathcal{F}^a(x,t)\,dx \equiv F_1^a(t) \quad \text{and} \quad \int\limits_0^1 \mathcal{F}^a(x,t)\,\frac{dx}{x} \equiv R_1^a(t), \tag{55}$$

and similarly for $\mathcal{K}, \mathcal{G}, \mathcal{P}$. The functions $F_1^a(t)$ are the flavor components of the usual $F_1(t)$ form factor while $R_1^a(t)$ are the flavor components of a new form factor specific to the wide-angle Compton scattering. In the formal asymptotic limit $|t| \to \infty$, the x integrals for $F_1^a(t)$ and $R_1^a(t)$ are both dominated in our model by the $x \sim 1$ region: the large-t behavior of these functions is governed by the Feynman mechanism and their ratio tends to 1 as $|t|$ increases (see Fig. 11a). However, due to large value of the effective scale $4\lambda^2 = 2.8$ GeV^2, the accessible momentum transfers $t < 5$ GeV^2 are very far from being asymptotic.

In Fig. 11b we plot $\mathcal{F}^u(x;t)$ and $\mathcal{F}^u(x;t)/x$ at $t = -2.5$ GeV^2. It is clear that the relevant integrals are dominated by rather small x values $x < 0.4$ which results in a strong enhancement of $R_1^u(t)$ compared to $F_1^u(t)$ for $|t| < 5$ GeV^2. Note also that the $\langle p'|\ldots x\hat{P}\ldots|p\rangle$ matrix elements can produce only t as a large variable while $\langle p'|\ldots\hat{Q}\ldots|p\rangle$ gives s. As a result, the enhanced form factors $R_1^a(t)$ are accompanied by extra s/t enhancement factors compared to the $F_1^a(t)$ terms. In the cross section, these enhancements are squared, *i.e.*, the contributions due to the non-enhanced form factors $F_1^a(t)$ are always accompanied by t^2/s^2 factors which are smaller than $1/4$ for cm angles below 90°. Because of double suppression, we neglect $F_1^a(t)$ terms in the present simplified approach.

The contribution due to the $\mathcal{K}$ functions appears through the flavor components $F_2^a(t)$ of the $F_2(t)$ form factor and their enhanced analogues $R_2^a(t)$. The major part of contributions due to the $\mathcal{K}$-type NDs appears in the combination $R_1^2(t) - (t/4m_p^2)R_2^2(t)$. Experimentally, $F_2(t)/F_1(t) \approx 1\,\text{GeV}^2/|t|$.

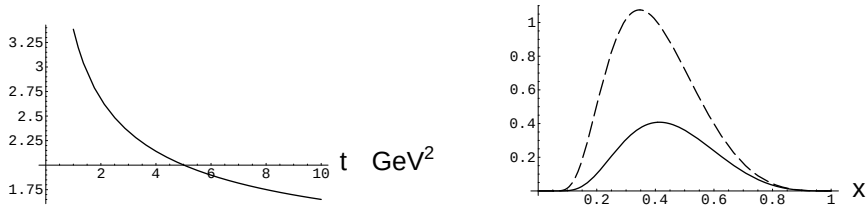

Fig. 11. a) Ratio $R_1^u(t)/F_1^u(t)$; b) Functions $\mathcal{F}^u(x;t)$ (solid line) and $\mathcal{F}^u(x;t)/x$ (dashed line) at $t=-2.5$ GeV^2.

Since $R_2/F_2 \sim R_1/F_1 \sim 1/\langle x\rangle$, $R_2(t)$ is similarly suppressed compared to $R_1(t)$, and we neglect contributions due to the $R_2^a(t)$ form factors. We also neglect here the terms with another spin-flip distribution $\mathcal{P}$ related to the pseudoscalar form factor $G_P(t)$ which is dominated by the t-channel pion exchange. Our calculations show that the contribution due to the parton helicity sensitive densities $\mathcal{G}^a$ is suppressed by the factor $t^2/2s^2$ compared to that due to the $\mathcal{F}^a$ densities. This factor only reaches $1/8$ for the cm angle of 90°, and hence the $\mathcal{G}^a$ contributions are not very significant numerically. For simplicity, we approximate $\mathcal{G}^a(x,t)$ by $\mathcal{F}^a(x,t)$. After these approximations, the WACS cross section is given by the product

$$\frac{d\sigma}{dt} \approx \frac{2\pi\alpha^2}{\tilde{s}^2}\left[\frac{(pq)}{(pq')}+\frac{(pq')}{(pq)}\right] R_1^2(t)\,, \tag{56}$$

of the Klein–Nishina cross section (in which we dropped $O(m^2)$ and $O(m^4)$ terms) and the square of the $R_1(t)$ form factor

$$R_1(t) = \sum_a e_a^2 \left[R_1^a(t) + R_1^{\bar{a}}(t)\right]\,. \tag{57}$$

In our model, $R_1(t)$ is given by

$$R_1(t) = \int_0^1 \left[e_u^2\, f_u^{\rm val}(x) + e_d^2\, f_d^{\rm val}(x) + 2(e_u^2+e_d^2+e_s^2)\, f^{\rm sea}(x)\right] \mathrm{e}^{\bar{x}t/4x\lambda^2}\,\frac{dx}{x}\,. \tag{58}$$

We included here the sea distributions assuming that they are all equal $f^{\rm sea}(x) = f^{\rm sea}_{u,d,s}(x) = f_{\bar{u},\bar{d},\bar{s}}(x)$ and using a simplified parametrization

$$f^{\rm sea}(x) = 0.5\, x^{-0.75}(1-x)^7 \tag{59}$$

which accurately reproduces the GRV formula for $Q^2 \sim 1$ GeV^2. Due to suppression of the small-x region by the exponential $\exp[\bar{x}t/4x\lambda^2]$, the sea

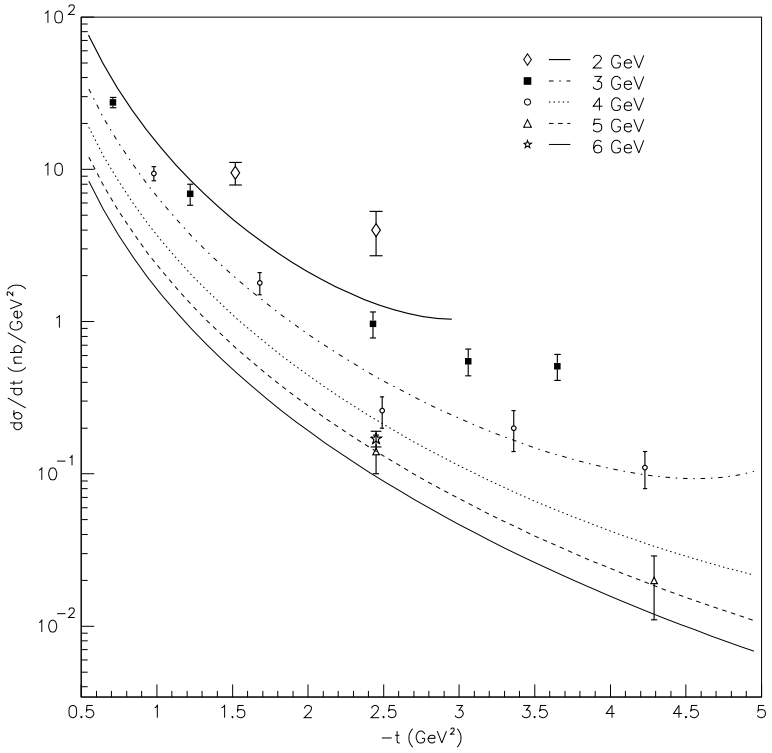

Fig. 12. WACS cross section versus t: comparison of results based on Eq. (56) with experimental data.

quark contribution is rather small ($\sim 10\%$) even for $-t \sim 1$ GeV^2 and is invisible for $-t > 3$ GeV^2.

Comparison with existing data [47] is shown in Fig. 12. Our curves follow the data pattern but are systematically lower by a factor of 2, with disagreement becoming more pronounced as the scattering angle increases. Since we neglected several terms each capable of producing up to a 20% correction in the amplitude, we consider the agreement between our curves and the data as encouraging. The most important corrections which should be included in a more detailed investigation are the t-corrections in the denominators of hard propagators and contributions due to the "non-leading" $\mathcal{K}, \mathcal{G}, \mathcal{P}$ nonforward densities. The latter, as noted above, are usually accompanied by t/s and t/u factors, *i.e.*, their contribution becomes more significant at larger angles. The t-correction in the most important hard propagator term $1/[x\tilde{u} - (\bar{x}^2 - \alpha^2)t/4 + x^2M^2]$ also enhances the amplitude at large angles.

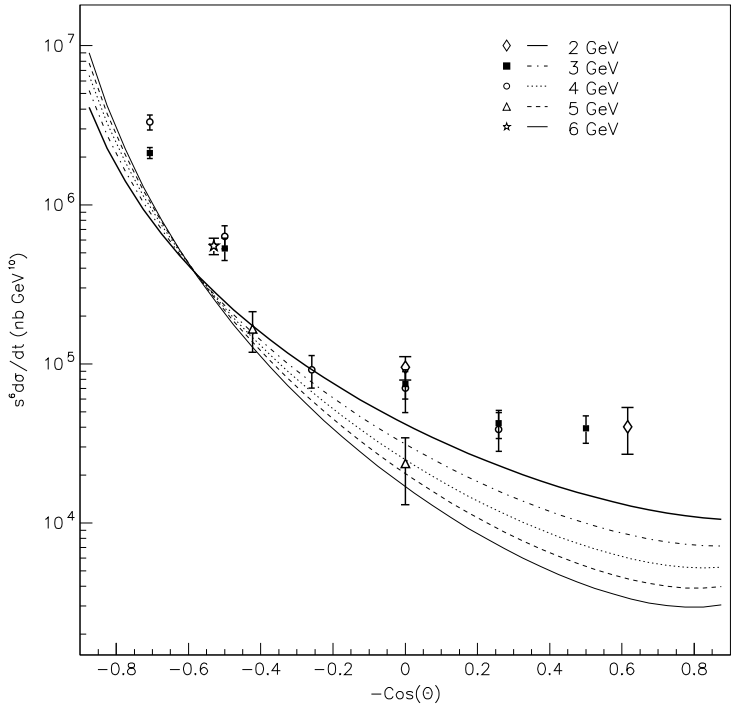

Fig. 13. Angular dependence of the combination $s^6(d\sigma/dt)$.

The angular dependence of our results for the combination $s^6(d\sigma/dt)$ is shown on Fig. 13. All the curves for initial photon ehergies 2,3,4,5 and 6 GeV intersect each other at $\theta_{\rm cm} \sim 60^\circ$. This is in good agreement with experimental data of Ref. [47] where the differential cross section at fixed cm angles was fitted by powers of s: $d\sigma/dt \sim s^{-n(\theta)}$ with $n^{\rm exp}(60^\circ) = 5.9 \pm 0.3$. Our curves correspond to $n^{\rm soft}(60^\circ) \approx 6.1$ and $n^{\rm soft}(90^\circ) \approx 6.7$ which also agrees with the experimental result $n^{\rm exp}(90^\circ) = 7.1 \pm 0.4$.

This can be compared with the scaling behavior of the asymptotic hard contribution: modulo logarithms contained in the α_s factors, they have a universal angle-independent power $n^{\rm hard}(\theta) = 6$. For $\theta_{\rm cm} = 105^\circ$, the experimental result based on just two data points is $n^{\rm exp}(105^\circ) = 6.2 \pm 1.4$, while our model gives $n^{\rm soft}(105^\circ) \approx 7.0$. Clearly, better data are needed to draw any conclusions here.

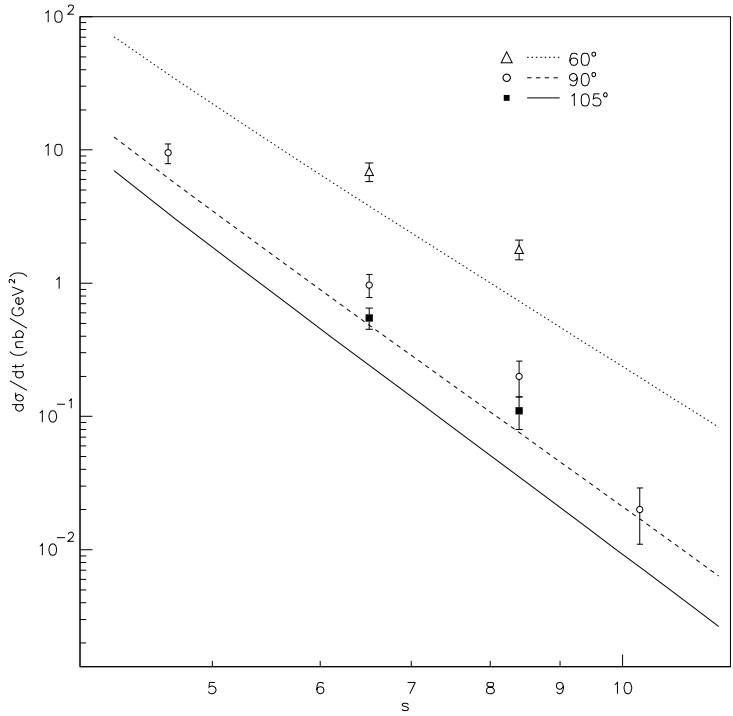

Fig. 14. s-dependence of the combination $s^6 d\sigma/dt$ for $\theta = 60°$ (dotted line), $\theta = 90°$ (dashed line) and $\theta = 105°$ (solid line).

9. Conclusions

The hard exclusive electroproduction processes provide new information about hadronic structure accumulated in skewed parton distributions. The SPDs are universal hybrid functions having the properties of parton densities, hadronic form factors and distribution amplitudes. They give a unified description of various hard exclusive and inclusive reactions. The basic supplier of information about skewed parton distributions is deeply virtual Compton scattering which offers a remarkable example of Bjorken scaling phenomena in exclusive processes. Furthermore, wide-angle real Compton scattering is an ideal tool to test angle-dependent scaling laws characteristic for soft overlap mechanism.

I am grateful to A. Białas and M. Praszałowicz for hospitality in Zakopane and support. I thank K. Golec-Biernat for discussions. This work was supported by the U.S. Department of Energy under Contract No. DE-AC05-84ER40150.

REFERENCES

[1] R.P. Feynman, *The Photon–Hadron Interaction*, Benjamin, Reading 1972.

[2] V.L. Chernyak, A.R. Zhitnitsky, *JETP Letters*, **25**, 510 (1977); V.L. Chernyak, A.R. Zhitnitsky, V.G. Serbo, *JETP Letters* **26**, 594 (1977).

[3] D.R. Jackson, Thesis, CALTECH, 1977 (unpublished); G.R. Farrar, D.R. Jackson, *Phys. Rev. Lett.* **43**, 246 (1979).

[4] A.V. Radyushkin, JINR report P2-10717, Dubna, 1977 (unpublished).

[5] A.V. Efremov, A.V. Radyushkin, JINR preprint E2-11983, Dubna (October 1978), published in *Theor. Math. Phys.* **42**, 97 (1980).

[6] S.J. Brodsky, G.P. Lepage, *Phys. Lett.* **87B**, 359 (1979).

[7] S.J. Brodsky, G.P. Lepage, *Phys. Rev.* **D22**, 2157 (1980).

[8] X. Ji, *Phys. Rev. Lett.* **78**, 610 (1997); *Phys. Rev.* **D55**, 7114 (1997).

[9] A.V. Radyushkin, *Phys. Lett.* **B380**, 417 (1996);

[10] A.V. Radyushkin, *Phys. Lett.* **B385**, 333 (1996).

[11] A.V. Radyushkin, *Phys. Rev.* **D56**, 5524 (1997).

[12] J.C. Collins, L. Frankfurt, M. Strikman, *Phys. Rev.* **D56**, 2982 (1997).

[13] D. Müller, D. Robaschik, B. Geyer, F.-M. Dittes, J. Hořejši, *Fortschr. Phys.* **42**, 101 (1994).

[14] J. Bartels, M. Loewe, *Z. Phys.* **C12**, 263 (1982).

[15] L.V. Gribov, E.M. Levin, M.G. Ryskin, *Phys. Rep.* **100**, 1 (1983).

[16] H. Abramowicz, L. Frankfurt, M. Strikman, *SLAC Summer Institute*, Stanford 1994, p. 539; hep-ph/9503437.

[17] A.V. Radyushkin, *Phys. Rev.* **D59**, 014030 (1999).

[18] A.V. Radyushkin, *Phys. Lett.* **B449**, 81 (1999).

[19] A.V. Radyushkin, Phys. Lett. **B131**, 179 (1983).

[20] M.V. Polyakov, C. Weiss, RUB-TPII-1-99, hep-ph/9902451.

[21] A.V. Radyushkin, *Phys. Rev.* **D58**, 114008 (1998).

[22] L. Mankiewicz, G. Piller, T. Weigl, *Eur. Phys. J.* **C5**, 119 (1998).

[23] X. Ji, *J. Phys. G* **24**, 1181 (1998).

[24] CLEO Collaboration (J. Gronberg *et al.*), *Phys. Rev.* **D57**, 33 (1998).

[25] M. Vanderhaeghen, P.A.M. Guichon, M. Guidal, *Phys. Rev. Lett.* **80**, 5064 (1998); *Phys. Rev.* **D60**, 094017 (1999); P.A.M. Guichon, M. Vanderhaeghen, *Prog. Part. Nucl. Phys.* **41**, 125 (1998).

[26] A.G. Shuvaev, K.J. Golec-Biernat, A.D. Martin, M.G. Ryskin, *Phys. Rev.* **D60**, 014015 (1999).

[27] I.V. Musatov, A.V. Radyushkin, hep-ph/9905376.

[28] X. Ji, J. Osborne, *Phys. Rev.* **D58**, 094018 (1998).

[29] J.C. Collins, A. Freund, *Phys. Rev.* **D59**, 074009 (1999).

[30] O. Nachtmann, *Nucl. Phys.* **B63**, 237 (1973).

[31] H. Georgi, H.D. Politzer, *Phys. Rev.* **D14**, 1829 (1976).

[32] S.J. Brodsky, T.Huang, G.P.Lepage, in *Particles and Fields 2*, Proceedings of the Banff Summer Institute, Banff, Alberta, 1981, edited by A.Z. Capri and A.N. Kamal, Plenum, New York 1983, p.143.

[33] M. Gluck, E. Reya, A. Vogt, *Z. Phys.* **C67**, 433 (1995).

[34] L. Andivahis *et al. Phys. Rev.* **D50**, 5491 (1994).

[35] B.L. Ioffe, A.V. Smilga, *Nucl. Phys.* **B232**, 109 (1984).

[36] I.I. Balitsky, A.V. Yung, *Phys. Lett.* **B129**, 328 (1983).

[37] V.A. Nesterenko, A.V. Radyushkin, *JETP Lett.* **39**, 707 (1984).

[38] V.M. Belyaev, Ya.I. Kogan, *Int. J. Mod. Phys.* **A8**, 153 (1993).

[39] I.I. Balitsky, *Phys. Lett.* **B114**, 53 (1982).

[40] M. Diehl, T. Feldmann, R. Jakob, P. Kroll, *Eur. Phys. J.* **C8**, 409 (1999).

[41] S.J. Brodsky, G.R. Farrar,*Phys. Rev. Lett.* **31**, 1153 (1973).

[42] V.A. Matveev, R.M. Muradyan, A.N. Tavkhelidze, Lett. Nuovo Cim. **7**, 719 (1973).

[43] G.R. Farrar, H. Zhang, *Phys. Rev.* **D41**, 3348 (1990); Erratum: *Phys. Rev.* **D42**, 2413 (1990).

[44] A. Kronfeld, B. Nižić, *Phys. Rev.* **D44**, 3445 (1991); Erratum: *Phys. Rev.* **D46**, 2272 (1992).

[45] M. Vanderhaeghen, DAPNIA-SPHN-97-42, Saclay (1997).

[46] A.V. Radyushkin, R. Ruskov, *Nucl. Phys.* **B481**, 625 (1996).

[47] M.A. Shupe *et al. Phys. Rev.* **D19**, 1921 (1979).